Available online at www.eccomasproceedia.org
Eccomas Proceedia COMPDYN (2025) 617- 628

ECCOMAS Proceedia

COMPDYN 2025
10th ECCOMAS Thematic Conference on
Computational Methods in Structural Dynamics and Earthquake Engineering
M. Papadrakakis, M. Fragiadakis (eds.)
Rhodes Island, Greece, 15-18 June 2025

A MULTI-OBJECTIVE OPTIMIZATION FRAMEWORK TOWARDS DERIVING OPTIMAL VISCOUS DAMPER PROPERTIES FOR BASE ISOLATED RC BUILDINGS CORRESPONDING TO DIFFERENT SEISMIC SCENARIOS

Subhra Das[1], and Sandip Das[1]

[1] Department of Civil Engineering, Indian Institute of Technology Guwahati, Guwahati, Assam, India-781039
e-mail: {das176104111, sandip.das}@iitg.ac.in

Abstract

In seismic engineering, designing optimal passive control systems is essential for enhancing structural resilience under varying ground motion scenarios. Although base isolation system reduces structural response quite effectively, yet use of viscous dampers in conjunction are proven to be complementary as viscous dampers offers additional damping and energy dissipation during long duration or extreme events. Viscous dampers have emerged as an effective means of reducing structural responses; however, deriving optimal properties of the viscous dampers still remains challenging due to the diversity and randomness of seismic excitations. Given, the inevitable occurrence of earthquakes of varying intensities over the lifetime of a structure, it becomes inherently essential to assess the structural performance under multiple anticipated seismic shaking levels pertaining to different seismic scenarios.

This paper presents a methodology for deriving the optimal viscous damper properties considering multiple levels of seismic shaking (viz. light, medium and severe) corresponding to different seismic scenarios. A multi-objective optimization framework towards optimizing the maximum inter-storey drift ratio based seismic risk for the three levels of shaking is proposed in this study. The isolation system comprises Lead Rubber bearings installed beneath each column to detach the superstructure from foundation. The superstructure, isolation system and viscous dampers are modeled in OpenSees as it supports modularity and fast computational performance. Analysis results reveal that the optimal properties of viscous damper mounted on the base isolated RC building corresponding to one shaking level fail to ensure satisfactory performance at other levels. In contrast the proposed multi objective frame work successfully identifies the optimal viscous damper properties for the base isolated RC building, capable of delivering satisfactory performance across all the considered seismic shaking levels. The proposed methodology provides engineers with a reliable tool for designing base isolated RC building frames with viscous dampers that is both effective and adaptable to complex seismic environments.

Keywords: Base isolation, Lead Rubber Bearing, Viscous Damper, Optimization, Seismic scenario.

Peer-review under responsibility of the organizing committee of COMPDYN 2025.
doi: 10.7712/120125.12678.25278

1 INTRODUCTION

The devastating impact of seismic forces on the buildings, infrastructure and human lives necessitates the introduction of innovative technologies to mitigate these impacts. Seismic isolation is proven to be an effective technique in mitigating earthquake induced forces on the structure. By introducing a flexible isolation layer at the base, the superstructure is decoupled from foundation which reduces the structural damage significantly and ensures occupant safety. The base isolation system reduces the seismic forces transmitted to the superstructure quite effectively by elongating the natural period of the structure and dissipating energy through hysteresis. Kelly [1] has carried out a detail investigation on the base isolation system and discussed about three types of isolation bearings viz. Lead Rubber bearing (LRB), High damping Rubber Bearing (HDRB) and Friction Pendulum Bearing (FPB). Amidst the three types of bearings, LRB has gradually secured its position since its inception in New-Zealand [2] as it provides additional energy dissipation through plastic deformation of the lead core.
Lead Rubber Bearings (LRBs) are a type of elastomeric bearing that primarily consists of alternating layers of elastomer i.e. rubber and steel shims along with a central lead core. The rubber layers ensure flexibility at the isolation level while the intermediate steel shims enhance vertical stiffness and prevent excessive compressive deformation. The central lead core efficiently dissipates energy while undergoing plastic deformation.

However, while the base isolation with LRBs effectively reduces seismic forces, it can lead to excessive displacements at the base especially during long duration earthquakes or near fault ground motions with strong velocity pulses posing challenges related to stability and serviceability [3]. This excessive displacement may cause significant damage to the isolation system and sometimes results in pounding with the adjacent structures. To counteract this issue, several researches [4-6] have reported the use of additional damping devices like metallic, friction; fluid, tuned mass and viscous dampers in base isolated structures. Out of these, the fluid viscous dampers (FVDs) are commonly used as: a) they offer significant seismic resistance via energy dissipation b) they can enhance the structure’s damping ratio without substantially modifying the inherent stiffness. Due to these key features, FVDs have gained attention as supplemental damping devices in base isolated structures. Besides, one added advantage is that the FVDs are less sensitive to a wider range of frequencies as well as temperatures.

Basically, FVDs are velocity dependent energy dissipation devices that generate resistance by transmitting a highly viscous fluid through an orifice of a sealed cylinder. Based on the velocity exponent, the FVDs can be categorized in two parts: Linear (velocity exponent=1) and non linear (velocity exponent<1). Some studies state that non linear FVDs are more efficient than their linear counterparts in terms of energy dissipation. In a study, Hall [8] has reported that the displacement demand of the isolation system and drift can be effectively reduced by incorporating additional damping. Other studies [9,10] have also mentioned about the significant advantages of using additional damping devices. Wolff et. al [11] provides details regarding some interesting applications of FVDs; they have also performed a comparative study of linear and non linear FVDs.

This paper presents a seismic risk based optimal design for FVD mounted base isolated (with LRB) RC building. Seismic risk corresponding to three levels of seismic shaking (viz. Light, Medium and Severe) considered on the basis of distinct magnitude values form the objectives for this present study. The ground motions generated under the seismic scenarios in this study consider both the source to site distance and focal depth as 8 km. The initial stiffness (K_i) and characteristic strength (Q_d) are chosen as the design variables for the LRB based isolation system as these are the most influential properties of LRB. Besides, the damping coefficient (C_d) and the velocity exponent (α_d) which determines the force velocity behavior of the viscous damper are also considered as the design variables along the LRB parameters.

2 MODELING OF THE BASE ISOLATED RC BUILDING WITH FVD

The base isolated RC building model considered in this study is a 5 storey building which is symmetric along both the horizontal directions. For the purpose of simplification, an internal 2D frame of the mentioned building has been considered during non linear dynamic analyses.

The building has uniform storey height of 3.0 m. Uniform column sections of 400 mm x 400 mm and uniform beam sections of 350 mm x 250 mm have been considered throughout the whole building. The column and beam sections are presented in Figure 1. The superstructure has been designed as per the provisions of the Indian design codes: IS 456 (2000) [12], IS 13920 (2016) [13], IS 1893 (2016) [14], and IS 875 (2008) Part-I [15] and Part-II [16]. For this purpose, M-25 grade of concrete (with characteristic cube strength f_{ck} as 25 MPa and Modulus of elasticity Ec as 25000 MPa) and Fe 500 grade steel (with characteristic yield strength f_y as 500 MPa and modulus of elasticity Es as 200 GPa) are considered. The frame has three bays, each having 4.0 m width. The finite element models are developed using OpenSees framework [17]. The cyclic strength degradation in the ReinforcingSteel material is modeled using the Giuffre-Menegotto-Pinto model [18]. The related parameters are taken as follows: f_y=500 MPa, f_u=600 MPa, E_s=200GPa, E_{sh}=10 GPa, ϵ_{sh}=0.005 and ϵ_u=0.12. The Concrete07 material is used to model the confined and un-confined concrete. Behaviour of the concrete is governed by Chang-Mander [19] stress strain relationships.

The beamWithHinges element is used to model the frame members which localizes plastic hinge at the element ends. The Paulay and Priestley [20] equation for reinforced concrete members can be used to find the length of the plastic hinges as follows:

$$l_p = 0.08L + 0.022 f_y d_b \qquad (1)$$

where, l_p is the length of plastic-hinge in metres, L represents the member shear-span in metres, f_y defines the yield strength of steel in MPa and d_b denotes the diameter of the longitudinal reinforcement in metres.

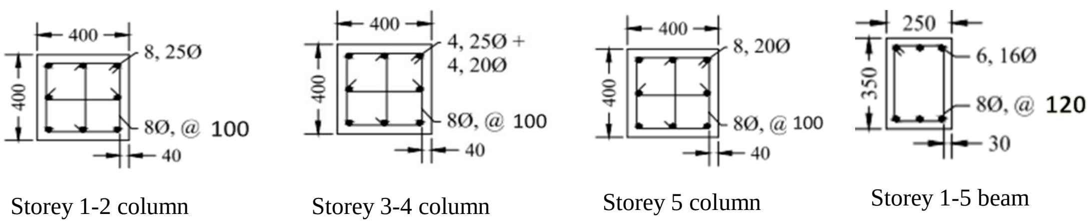

Figure 1: Beam and column sections of the considered building

The isolation system is considered to contain the Lead Rubber Bearings (LRBs), which are the most common types of isolators in practice [21,22]. The LRBs are placed beneath the columns of the superstructure. The elastomericBearingBoucWen element is used to model the LRBs. Since the initial stiffness (K_i) and the characteristic strength (Q_d) are two most influential parameters which characterize the force displacement behaviour of LRB, these two parameters are chosen as the design variables. The post yield stiffness ratio for linear hardening (α_1) and non linear hardening component (α_2) are taken as 0.1 and 0.0 respectively. The catalogue of Dynamic Isolation System [23] provides the feasible range of the post elastic stiffness (Kd) and characteristic strength (Qd) based on the axial load as 0.4-0.7 kN/mm and 0-

180 kN, respectively. The elastic stiffness is estimated by $K_i = \frac{K_d}{\alpha_1}$ (as α_2=0.0). The exponent of non-linear hardening component (μ) is taken as 1.0 while the yielding exponent (h) is considered to be 10.0 to accurately capture the residual deformation. Besides, the first (β) and second (g) hysteretic shape parameters are considered as 0.5 and 0.5 respectively. With the knowledge of K_i, K_d and Q_d, the yield displacement (D_y) and the yield strength (F_y) can be estimated as follows [24]:

$$D_y = \frac{Q_d}{K_i - K_d} \qquad (2)$$

$$F_y = K_i \times D_y \qquad (3)$$

The typical hysteretic behavior of LRB is presented in figure 2

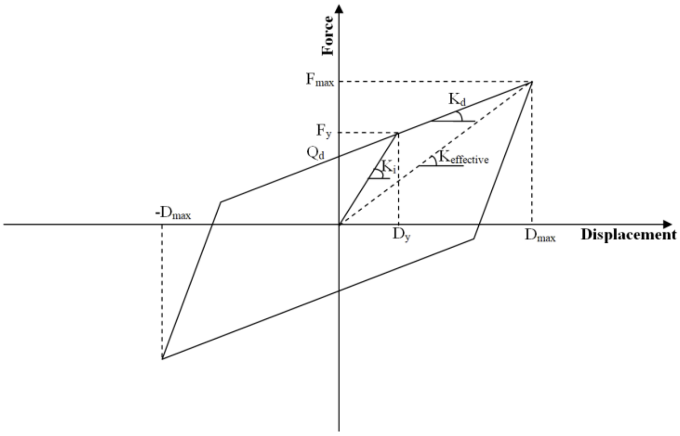

Figure 2: Hysteretic behavior of LRB

One of the significant benefits of non linear FVD is its capability to restrain the forces exerted on the damper, allowing for efficient dissipation of seismic energy [10]. Two essential parameters namely, damping coefficient (C_d) and velocity exponent (α_d) characterize the damper force, which can be computed as [11]:

$$F_d = C_d v^{\alpha_d} sign(v) \qquad (4)$$

Where, F_d is the damper force, v denotes the velocity of the damper, α_d represents the velocity exponent, and sign(.) is the signum function. Keeping this in mind, the damping coefficient (C_d) and velocity exponent (α_d) are selected as the design variables along with the other two design variables (K_i and Q_d) of LRB. In accordance with Liu, Wu and Dona [25], the feasible range of damping coefficient (C_d) is taken as 1-10^7 N$(s/m)^{\alpha_d}$ and velocity exponent (α_d) is taken as 0.1-1.0. The nonlinear FVDs are modeled in OpenSees. Following the approach in [26], the FVDs are placed in the middle bay of all the stories. The gravity loading details of the FVD mounted 5-storey base isolated RC building frame considered in this study is presented in figure 3.

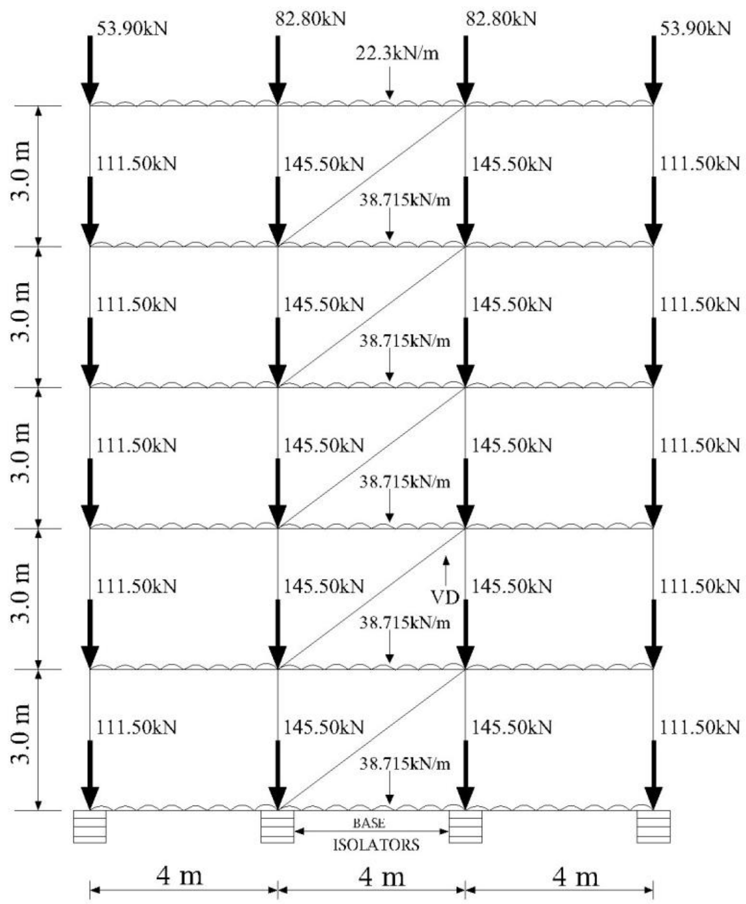

Figure 3: Gravity loading details of the 5-storey isolated frame with FVD

3 PROPOSED MULTI LEVEL SHAKING BASED FRAMEWORK

3.1 Generation of input ground motions

Anderson and Bertero [27] have demonstrated that the structural response characteristics significantly vary with ground motions occurred at site to site. Again, FEMA P-58 states "scenario based assessments evaluate the probable performance of a building assuming that it is subjected to an earthquake scenario consisting of a specific magnitude earthquake, occurring at a specific location relative to the building site".

In view of the above, ground motions pertaining to different scenarios are generated (listed in table 1) due to Nithin et al. [28]. Under each listed scenario 20 ground motions are generated. The generated scenarios are classified into three scenario classes (viz. Light, Medium, Severe) based on the magnitude. Though the magnitudes are chosen hypothetically, they are consistent for light (smallest) to severe (largest) events. Apart from that, both the source to site distance and focal depth are taken as 8 km. Two types of soil conditions are considered, soft soil and rock. Twenty ground motions are generated under each scenario. Figure 4 presents the response spectra for the weakest scenario i.e. scenario L2 and the most severe scenario i.e. scenario S1 (identified on the basis of median PGA). The median of the respective spectra are shown in bold blue dotted lines.

Scenario class	Scenario Label	Magnitude	Source to Site Distance (km)	Focal Depth (km)	Soil Type
Light	L1	5	8	8	Soft soil
	L2	5	8	8	Rock
Medium	M1	6	8	8	Soft soil
	M2	6	8	8	Rock
Severe	S1	7.3	8	8	Soft soil
	S2	7.3	8	8	Rock

Table 1: Description of generated ground motions.

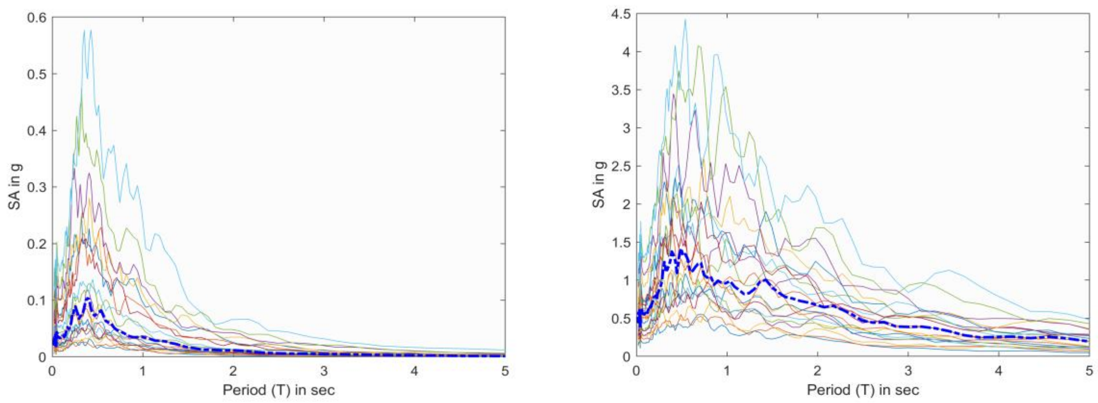

(a) Scenario L2 (weakest scenario) (b) Scenario S1 (most severe scenario)

Figure 4: Response spectra plots of scenarios L2 and S1

3.2 Multi objective optimization model

The deterministic seismic risk is considered as the performance measure for the objective functions. For each scenario, individual 20 responses in the form of maximum interstorey drift ratio (MIDR) have been obtained through time history analysis and maximum likelihood estimation is used to fit lognormal distribution on the responses. The Interstorey Drift Ratio (IDR) based limit states are adopted from Hazus [29]. Since, the anticipated target performance levels are different for different levels of seismic shaking; different limit states have been adopted against different shaking levels. The limit states are presented in table 2.

Scenario class	Limit State Label	IDR Limit for risk calculation
Light	LS-L	0.0033
Medium	LS-M	0.0058
Severe	LS-S	0.0156

Table 2: Considered limit states from Hazus [28]

MCEER 15-005 [30] and ASCE 7-22 [31] recommend bounding analysis of the LRB properties to account for various issues like heating of the lead core, scragging, aging etc. which, in fact influence the mechanical properties of the LRB over time. Consequently, bounding analysis of the nominal properties of the LRB (i.e. K_i and Q_d) is performed during seismic risk calculation.

The multi-objective optimization model is expressed as:

$$x^* = \arg \min_{x \in X} \left(R^{Light}(x), R^{Medium}(x), R^{Severe}(x) \right) \quad (5)$$

$$\text{s.t.} \quad x_{\min} \le x \le x_{\max}$$

Where, $R^{Light}(.)$, $R^{Medium}(.)$ and $R^{Severe}(.)$ represent the seismic risk values corresponding to the Light, Moderate and Severe earthquake events. x is a feasible decision vector containing random values of $\{K_i, Q_d, C_d, \alpha_d\}$ within the decision vector space X. x^* represents the optimal solution; x_{min} and x_{max} correspond to $\{K_{i,min}, Q_{d,min}, C_{d,min}, \alpha_{d,min}\}$ and $\{K_{i,max}, Q_{d,max}, C_{d,max}, \alpha_{d,max}\}$, respectively.

3.3 Results and discussion

The Non-dominated sorting Genetic Algorithm-II (NSGA-II) [32] is one of the most popular algorithms for implementing multi objective optimization framework. Therefore, it is utilized to evaluate the proposed multi-objective optimization framework. For this purpose, population size of 100 and maximum generation limit of 20 are considered. It is observed that desired convergence is achieved with these values. In order to improve convergence while maintaining diversity, Simulated Binary Crossover (SBX) and polynomial mutation are incorporated.

Nonlinear dynamic analyses are performed using the generated ground motions (refer to table 1) during the optimization process. In order to see whether the optimal design properties corresponding to one shaking level can render optimal performance against other shaking levels with respect to respective associated target performance, the individual optimal properties of scenarios L1, M1, and S1 are derived and presented in table 3. Here onwards, the individual optimal risk for each scenario is referred to as the reference risk for that scenario. These scenarios are selected to represent distinct shaking levels (only on the basis of magnitude) while their soil condition, source to site distance and focal depth are kept same to represent a single building site.

Further, table 3 also presents the risk values corresponding to the remaining scenarios using the optimal properties of one scenario. It is not hard to see that the optimal parameters corresponding to one shaking level cannot yield optimal performance against the remaining ones. E.g. the optimal parameters for scenario S1 (severe level) produce large increase (96.78%) in risk value for scenario L1 (light level) and vice versa (i.e. 87.11% increase in risk value against scenario S1 while using optimal parameters corresponding to scenario L1). Similar results can be seen for other scenarios too. Hence, it is imperative that no such stringent case exists whose optimal properties can render optimal performance or at least near optimal performance for the remaining scenarios (or shaking levels). Thus, a multi-objective framework with multiple shaking levels is necessary as a structure is basically designed considering multiple shaking levels and their associated target performance. Typically a building site is selected in prior to the design of the building. Keeping this in mind, the scenarios presented in table 1 are classified into two site classes, namely, class-A and class-B. For better readability, the site class details are presented in table 4.

Scenario	Optimal values of design variables	Optimal seismic risk (reference risk)	Risk values against other scenarios (with % of increase from reference risk)	
			Scenario-M1	Scenario-S1
L1	K_i=6.481 kN/mm, Q_d= 83.29 kN, C_d= 4.1×10^5 $N(s/m)^{\alpha_d}$, α_d=0.2533	0.103472	0.244762 (67.24% increase)	0.389625 (87.11% increase)
			Scenario-L1	Scenario-S1
M1	K_i=5.193 kN/mm, Q_d= 54.26 kN, C_d= 4.7×10^5 $N(s/m)^{\alpha_d}$, α_d=0.2147	0.146354	0.188516 (82.19% increase)	0.363429 (74.53% increase)
			Scenario-L1	Scenario-M1
S1	K_i=4.527 kN/mm, Q_d= 40.72 kN, C_d= 5.5×10^5 $N(s/m)^{\alpha_d}$, α_d=0.1518	0.208233	0.203612 (96.78% increase)	0.228722 (56.28% increase)

Table 3: Optimal properties corresponding to different scenarios

Site class	Scenarios	Source to site distance (km)	Focal depth (km)	Soil condition
Class-A	L1, M1, S1	8	8	Soft soil
Class-B	L2, M2, S2	8	8	Rock

Table 4: Segregation of scenarios into site classes

The Pareto optimal fronts corresponding to Class-A and Class-B scenarios are presented in figure 5 and 6 respectively.

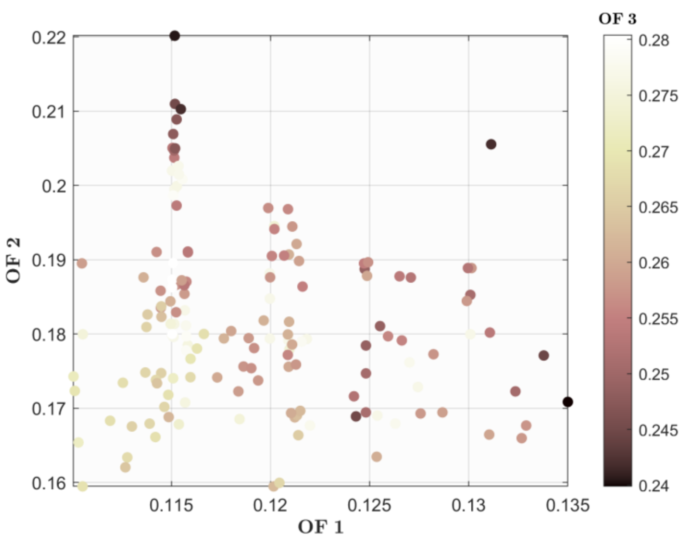

Figure 5: Pareto optimal front corresponding to scenarios L1, M1 & S1

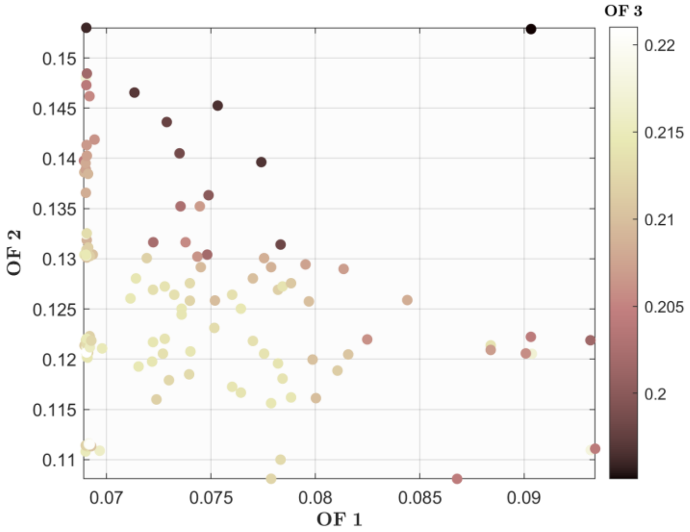

Figure 6: Pareto optimal front corresponding to scenarios L2, M2 & S2

In order to select a single efficient solution from the set of Pareto optimal solution, the Grey Relational Analysis (GRA) is utilized. The site class wise optimal values of design variables are presented in table 5. The optimal risk values corresponding to a site class is presented in the rightmost three columns. It can be easily observed from that the optimal parameters differ from site class to site class.

Site class	Optimal K_i (kN/mm)	Optimal Q_d (kN)	Optimal C_d $(10^5 \times N(s/m)^{\alpha_d})$	Optimal α_d	Optimal risk values		
					Light	Medium	Severe
Class-A (Scenario: L1, M1 & S1)	5.041	46.83	5.5143	0.1627	0.1243	0.1689	0.2449
	Percentage increase w.r.t. reference risk				20.13%	15.41%	17.61%
Class-B (Scenario: L2, M2 & S2)	6.283	57.26	4.6284	0.3583	0.0748	0.134	0.2019
	Percentage increase w.r.t. reference risk				16.35%	19.07%	15.82%

Table 5: Optimal design variables derived after performing GRA

When compared to the reference risk values, it is seen that the proposed multi objective framework is able to limit the percentage increase in risk values within 20.13% and 19.07% for the site class-A and B, respectively.

4 CONCLUSIONS

A seismic risk based multi-objective optimization framework considering multiple seismic shaking levels to derive the optimal fluid viscous damper and LRB properties is presented in this paper. The influential FVD parameters like damping coefficient, velocity exponent and key LRB parameters such as initial stiffness and characteristic strength are chosen as the design variables. Six different scenarios pertaining to three distinct scenario classes viz. Light, Medium and Severe are considered as seismic input. It is observed that the optimal risk values for all the three scenarios under site class-A (i.e. soft soil site) are higher compared to those under site class-B (rock site) which signifies the effect of soil condition on the performance of the FVD mounted base isolated RC building. It is also observed that the optimal values of design variables corresponding to one scenario cannot render optimal performance for the remaining scenarios which emphasizes the necessity of the proposed multi objective framework. Results reveal that the proposed multi-objective framework is capable of finding optimum solution that performs well across all the scenarios under a site class.

REFERENCES

[1] J.M. Kelly, D. Konstantinidis, *Mechanics of rubber bearings for seismic and vibration isolation.* New York, USA: John Wiley & Sons; 2011.

[2] N. Makris, Seismic isolation: Early history. *Earthquake Engineering and Structural. Dynamics.* **48**(2), 269-283, 2019.

[3] E.A. Mavronicola, P.C. Polycarpou, P. Komodromos, Effect of ground motion directionality on the seismic response of base-isolated buildings pounding against adjacent structures. *Engineering Structures*, **207**, 110202, 2020.

[4] C.G. Koh, T. Balendra, Seismic response of base isolated buildings including P-delta effects of isolation bearings. *Earthquake Engineering & Structural Dynamics*, **18**(4), 461-473, 1989.

[5] N. Markis, Rigidity –plasticity-viscosity: can electro-rheological dampers protect base-isolated structures from near-source ground motions. *Earthquake Engineering & Structural Dynamics*, **26**, 571-591, 1997.

[6] N. Makris, S. Chang, Effects of damping mechanisms on the response of seismically isolated structures. *PEER report 1998/06, Pacific Earthquake Engineering Research Center*, College of Engineering, University of California, Berkeley, CA: 1998.

[7] J.M. Kelly, Role of damping in seismic isolation. *Earthquake Engineering & Structural Dynamics*, **28**, 3-20, 1999.

[8] J. Hall, The role of damping in seismic isolation. *Earthquake Engineering & Structural Dynamics*, **28**, 1717-1720, 1999.

[9] M Fathi, A Makhdoumi, M Parvizi, Effect of supplemental damping on seismic response of base isolated frames under near & far field accelerations. *ASCE journal of Civil Engineering*, **19**(5), 1359-1365, 2015.

[10] CP Providakis, Effect of supplemental damping on LRB and FPS seismic isolators under near-fault ground motions. *Soil Dynamics and Earthquake Engineering,* **29**, 80-90, 2009.

[11] E.D. Wolff, C .Ipek, M.C. Constantinou, M. Tapan, Effect of viscous damping devices on the response of seismically isolated structures. *Earthquake Engineering & Structural Dynamics*, **44**, 185–98, 2015.

[12] IS 456, *Indian Standard: Plain and reinforced concrete - code of practice*, Bureau of Indian Standards, 2000.

[13] IS 13920, *Indian Standard: Code of practice for ductile detailing of concrete structures subjected to seismic forces*, Bureau of Indian Standards, 2016.

[14] IS 1893, *Indian Standard: Criteria for earthquake resistant design of structures -part 1: General provisions and buildings*, Bureau of Indian Standards, 2016.

[15] IS 875, *Code of practice for design loads (other than earthquake) for buildings and structures (Part 1: Dead loads unit weight of building materials and stored materials), Standard*, Bureau of Indian Standard: New Delhi, India, 2008.

[16] IS 875, *Code of practice for design loads (other than earthquake) for buildings and structures (Part 2: Imposed loads), Standard*, Bureau of Indian Standard: New Delhi, India, 2008.

[17] S. Mazzoni, F. McKenna, M. H. Scott, G. L. Fenves, *Opensees command language manual*. Technical report, Pacific Earthquake Engineering Research (PEER) Center, 2009.

[18] M. Manengotto, Method of Analysis for Cyclically Loaded Reinforced Concrete Plane Frames Including Changes in Geometry and Nonelastic Behviour of Elements under Combined Normal Force and Bending. *In IABSE Symposium on Resistance and Ultimate Deformability of Structures Acted on by Well-Defined Repeated Loads, Final Report*, **6(3)**, 266-272, 1973.

[19] G. Chang, and J.B. Mander, *Seismic energy based fatigue damage analysis of bridge columns: Part 1- evaluation of seismic capacity*. NCEER Technical Report. No. NCEER-94-0006, State University of Newyork, Buffalo, 1994.

[20] T. Paulay, and M. J.N. Priestly, *Seismic Design of Reinforced Concrete and Masonry Buildings*. John Wiley Sons, Inc, 2009.

[21] C. Li, K. Chang, L. Cao, and Y. Wang, Performance of a nonlinear hybrid base isolation system under the ground motions. *Soil Dynamics and Earthquake Engineering*, **143**, 1–15, 2021.

[22] G.J Hu, K. Ye, and Z.Y. Tang, Design and analysis of LRB base-isolated building structure for multilevel performance targets. *Structures*, **57**, 1–11, 2023.

[23] Dynamic isolation system: Seismic Isolation. https://www.dis-inc.com/brochures.html. Last Accessed January 15, 2025.

[24] H.N. Faal, and M. Poursha, Applicability of the N2, extended N2 and modal pushover analysis methods for the seismic evaluation of base-isolated building frames with lead rubber bearings (LRBs). *Soil Dynamics and Earthquake Engineering*, 98, 84–100, 2017.

[25] Y. Liu, J. Wu, and M. Dona, Effectiveness of fluid viscous dampers for improved seismic performance of inter-storey isolated buildings. *Engineering Structures*, 169, 276-292, 2018.

[26] M. Noruzvand, M. Mohebbi, and K. Shakeri, Modified direct displacement-based design approach for structures equipped with fluid viscous damper. *Structural Control & Health Monitoring*, **27**, e2465, 2020.

[27] J.C. Anderson, and V V Bertero, Uncertainties In Establishing Design Earthquakes. *ASCE Journal of Structural Engineering*, **113(**8), 1987.

[28] V.L. Nithin, S. Das, and H.B. Kaushik, Wavelet-based simulation of scenario-specific nonstationary accelerograms and their GMPE compatibility. *Soil Dynamics and Earthquake Engineering*, **99**, 56–67, 2017.

[29] HAZUS®MH MR4, *Multi-hazard Loss Estimation Methodology*, *Earthquake Model*, *Technical Manual*. Technical report, Federal Emergency Management Agency, 2003.

[30] W.J. McVitty, and M.C. Constantinou. *MCEER 15-005: Property Modification Factors for Seismic Isolators: Design Guidance for Buildings,* University at Buffalo, 2015.

[31] *ASCE/SEI 7-22: Minimum Design Loads and Associated Criteria for Buildings and Other Structures*, American Society of Civil Engineers, 2022.

[32] K. Deb, A. Pratap, S. Agarwal, and T. Meyarivan, A Fast and Elitist Multiobjective Genetic Algorithm: NSGA-II. *IEEE Transactions on Evolutionary Computation*, **6**(2), 182–197, 2002.